DESIGN AND SIMULATION OF AN ADVANCED BATTERY MANAGEMENT SYSTEM FOR ELECTRIC VEHICLE APPLICATIONS USING MATLAB/SIMULINK

[1]Varikuppala Manohar, [2]B.Ramakoti

[1]Postgraduate Student, [2]Associate Professor
[1]Department of Power & Industrial Drives,
[1]Dr.Paul Raj Engineering College, Bhadrachalam, India

Abstract : This paper presents the design, modeling, and simulation of a comprehensive Battery Management System (BMS) for electric vehicle (EV) applications, developed within the MATLAB/Simulink environment using Simscape physical modeling libraries. The proposed BMS architecture integrates a multi-module lithium-ion battery pack consisting of ten series-connected module assemblies, each containing two parallel cell strings, achieving a nominal pack voltage of approximately 420–440 V. Key BMS functionalities implemented and validated include: (1) State of Charge (SoC) estimation via an Adaptive Extended Kalman Filter (AEKF) operating on a first-order Thevenin equivalent circuit (1TC) cell model; (2) Overcurrent (OC) and Overdischarge (OD) current protection with adaptive current limits derived from real-time temperature and voltage measurements; (3) Thermal management through a closed-loop Battery Coolant Control algorithm that modulates coolant flow rate; (4) A hierarchical Fault Protection state machine that monitors voltage, current, temperature, and SoC thresholds, trips charge/discharge relays for one second per fault occurrence, and permanently disconnects the pack upon five cumulative electrical faults; and (5) A Relay Operation controller managing the main battery relay, charge relay, and discharge relay. Simulation results over a representative 130-second drive-and-charge cycle demonstrate stable SoC operation in the range 0.70–0.72, pack voltage between 362 V and 441 V, and temperature rise from 298.2 K to 300.1 K, with all protection functions operating correctly within their specified thresholds.

IndexTerms **– Battery Management System, Electric Vehicle, State of Charge, Fault Protection. Thermal Management**

I. INTRODUCTION

The rapid global proliferation of electric vehicles (EVs) has intensified research into the safe, reliable, and efficient management of high-energy lithium-ion (Li-ion) battery packs. A Battery Management System (BMS) serves as the central intelligence unit responsible for monitoring and controlling battery state variables—including voltage, current, temperature, and State of Charge (SoC)—to ensure operation within safe limits, maximize service life, and prevent catastrophic failures such as thermal runaway, deep discharge, or overcharge [1].

Modern BMS designs must simultaneously satisfy stringent requirements: high-accuracy SoC estimation across wide temperature and current ranges, rapid fault detection and isolation, thermal regulation under dynamic load profiles, and seamless coordination of charge and discharge relays [2]. Model-based development using MATLAB/Simulink and the Simscape physical modeling toolbox has emerged as the preferred methodology for BMS prototyping, enabling rapid algorithm development, hardware-in-the-loop (HIL) testing, and direct automatic code generation for embedded targets [3].

This paper describes a complete BMS simulation for a 420–440 V nominal EV pack organized around five functional subsystems: SoC Estimation (AEKF), Current Protection (OD/OC), Thermal Management, Fault Protection, and Relay Operation. The simulation is driven by a representative 130-second mission profile encompassing charging, resting, and dynamic load discharge events. The remainder of this paper is organized as follows: Section II reviews related work; Section III describes the battery pack architecture; Section IV details SoC estimation; Sections V–VII present current protection, thermal management, and fault protection; Section VIII discusses simulation results; Section IX concludes

II. RELATED WORK

A substantial body of literature addresses individual BMS functions. SoC estimation has been treated by coulomb counting [5], OCV lookup [6], and model-based filtering methods [7]. Among filtering approaches, the Extended Kalman Filter (EKF) [8] and its adaptive variant (AEKF) [9] have gained wide acceptance for their ability to handle nonlinear cell chemistry and online noise covariance tuning. The Unscented Kalman Filter (UKF) [10] and Particle Filter (PF) [11] offer improved accuracy at the cost of higher computational demand.

Thermal management of Li-ion packs has been investigated for liquid cooling [12], air cooling [13], and phase-change material (PCM) approaches [14]. Closed-loop coolant flow rate control based on cell temperature feedback is a practical and widely deployed strategy in automotive packs [15]. Fault detection and protection strategies range from threshold-based methods [16] to model-based observers [17] and data-driven approaches [18]. Relay-based isolation with a fault counter and manual reset mechanism is a standard automotive-grade protection scheme mandated by safety standards such as ISO 26262 and IEC 62619.

While individual BMS functions are well-studied, integrated simulation frameworks that simultaneously model the battery pack physics, SoC estimation, current limits, thermal control, and fault protection within a single Simulink environment are less commonly reported. This work contributes such an integrated framework, validated against a realistic mission profile, serving as a reference architecture for BMS algorithm development and code generation

III. SYSTEM ARCHITECTURE AND BATTERY PACK MODEL

3.1Top-Level Model Organization

The top-level Simulink model, illustrated in Fig. 1, comprises six primary subsystems interconnected via Simulink buses and Simscape physical connections: (1) Pack — the electrochemical and thermal battery model; (2) Sensor — signal conditioning and measurement; (3) BMS — the management controller; (4) Charger CC/CV — a constant-current/constant-voltage charging source; (5) Load — a controlled resistive discharge load; and (6) Controlled Mass Flow Rate Source — the thermal coolant actuator. Dashboard instruments including battery command switches, lamp indicators, warning panels, and real-time plotters are hosted in Simulink's dashboard environment.

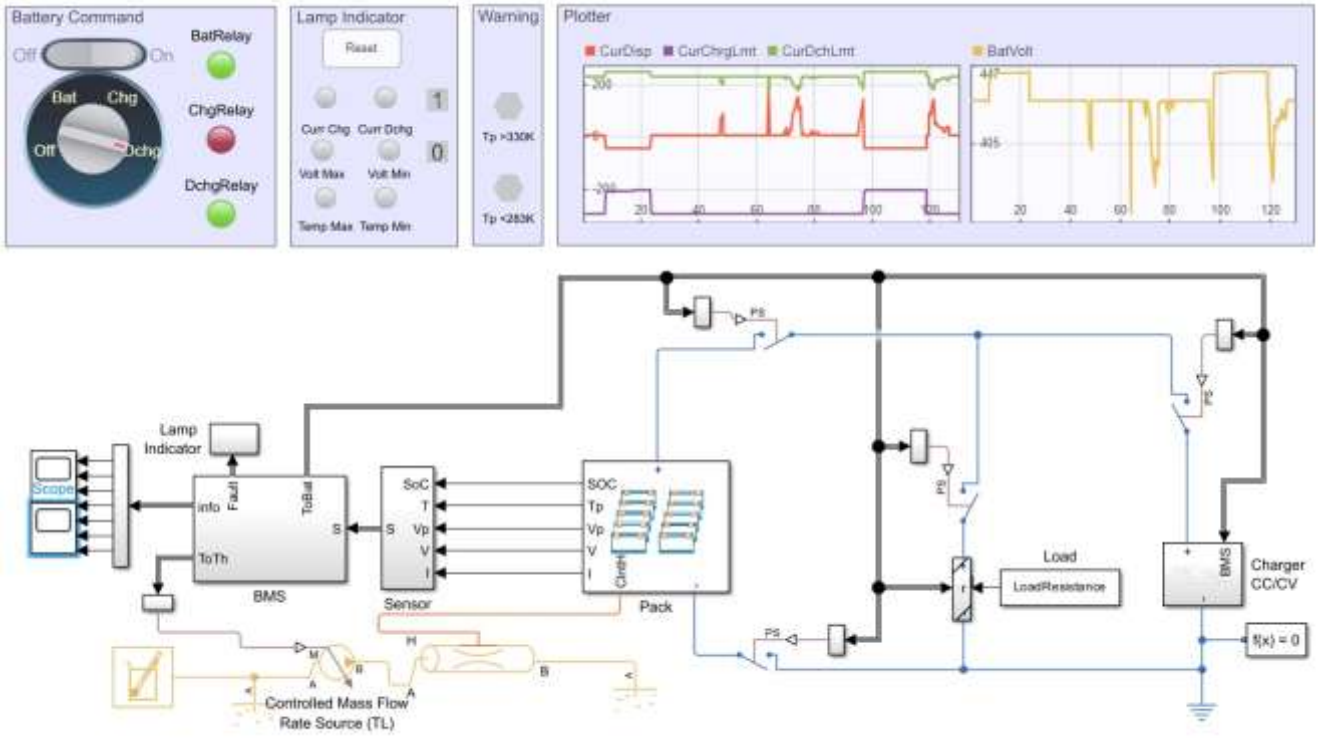

Fig. 1. Top-level MATLAB/Simulink model of the Battery Management System for electric vehicle application, showing the BMS controller, Sensor, Pack, Charger CC/CV, Load subsystems, and the interactive dashboard with real-time plotters.

3.2 Battery Pack Architecture

The battery pack is assembled from ten module assemblies (M1–M10) arranged in a 10S2P configuration — ten modules in series, each containing two cells in parallel — yielding a nominal pack voltage of 420–440 V. This topology is illustrated in Fig. 2. The Simscape Battery library models each cell using a parameterized equivalent-circuit model with temperature-dependent open-circuit voltage (OCV) look-up, internal resistance, and a first-order RC polarization network. The thermal network couples all cells to a common thermal bus representing the coolant circuit.

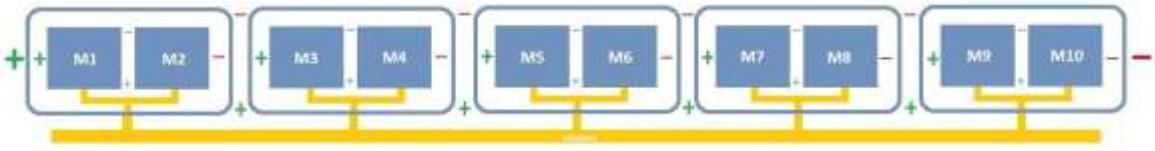

Fig. 2. Battery pack architecture showing ten series-connected module assemblies (M1–M10), each module containing two parallel cells, all sharing a common thermal bus for coolant-coupled thermal management.

Fig. 3 shows the full Simulink top-level schematic including the Charger CC/CV block, load resistance, relay switching network, and thermal connections. The Simscape physical connections (blue lines) carry electrical power, while orange lines carry thermal flux to the coolant mass flow source.

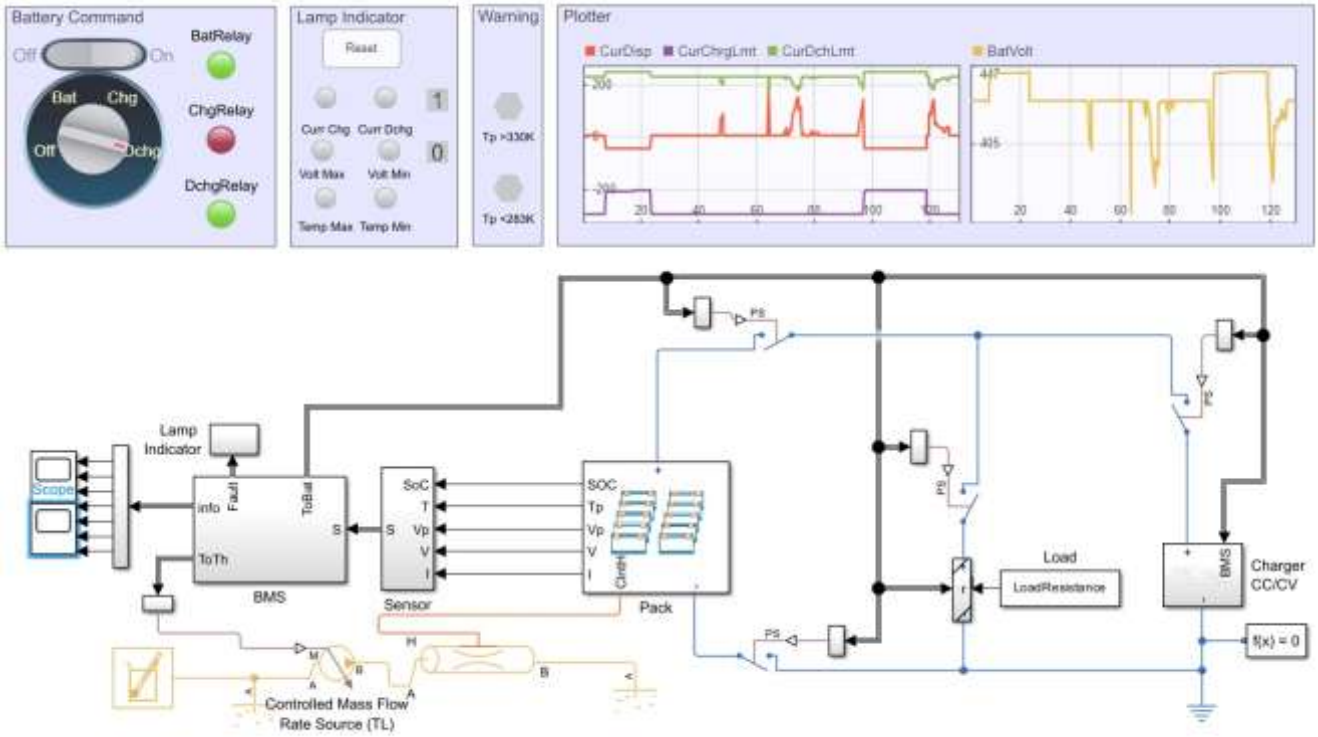

Fig. 3. Full Simulink/Simscape top-level schematic showing battery Pack, Charger CC/CV, Load, relay network, and Controlled Mass Flow Rate Source interconnections

3.3 Pack Subsystem – Internal Module Structure

Fig. 4 reveals the internal structure of the Pack subsystem, comprising five series-connected ModuleAssembly blocks (ModuleAssembly1–5), each exporting cell-level signals (iCell, nCyclesCell, socCell, socParallelAssembly, temperatureCell, vCell, vParallelAssembly) to the Sensor bus. Each module also connects to its respective thermal interface port (CIntH_1 through CIntH_5) for coolant heat exchange.

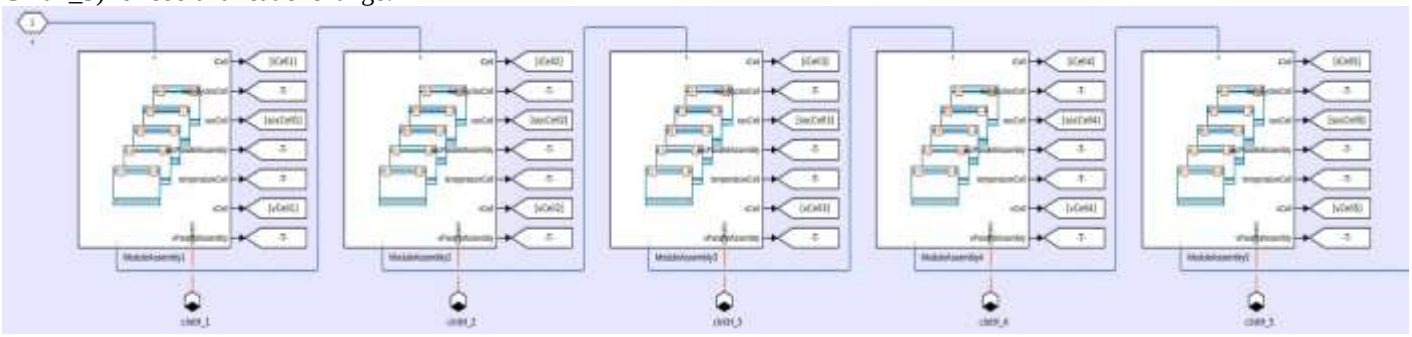

Fig. 4. Internal structure of the Pack subsystem showing five series-connected ModuleAssembly blocks with cell-level signal exports (SoC, current, voltage, temperature) and thermal interface ports

3.4 Key Parameters

Table 3.1: Key Parameters

Parameter	Value	Description
Configuration	10S2P	10 series × 2 parallel cells
Nominal Voltage	420-440V	Pack terminal voltage at 70% SoC
Discharge Current Limit	~225A	Current Discharge Limit (temperature dependent)
Charge Current Limit	~220A	Current Charge Limit (temperature dependent
Temp Warn Range	280-330 K	Tp Low Warning/ Tp High Warning
SoC Operating Window	0.698-0.723	Observed in 130 s Simulation
Temperature Rise	298.2 → 300.1K	+1.9 K over 130 s Simulation

IV. STATE OF CHARGE ESTIMATION

4.1 Cell Equivalent Circuit Model

The SoC estimation subsystem implements a first-order Thevenin equivalent circuit (1TC) observer. The cell terminal voltage is expressed as:

$$V_t = OCV(SoC,T) - I.R_o(SoC,T) - V_{RC}(t) \quad (4.1)$$

Where VRC is governed by the RC branch dynamics:

$$\frac{dV_{RC}}{dt} = -\frac{V_{RC}}{(R_1.C_1)} + \frac{I}{C_1} \quad (4.2)$$

All parameters (OCV, Ro, R1, C1) are represented as look-up tables over SoC and temperature, extracted from characterization data.

4.2 Adaptive Extended Kalman Filter (AEKF)

The AEKF operates on the augmented state vector x= [SoC, V_{RC}]^T . The discrete-time process and measurement models are:

$$x_{\{k+1\}} = f(x_k, I_k) + w_k \quad (4.3)$$

$$y_k = h(x_k, I_k) + v_k \quad (4.4)$$

where w_k ~ N(0, Q) and v_k ~ N(0, R) are the process and measurement noise, respectively. The adaptive variant updates Q and R online using an innovation-based covariance matching technique, improving robustness under varying current magnitudes and temperatures [9]. Current entering the AEKF block is scaled by gain −K to convert pack-level current to single-cell equivalent. Outputs CellSocMin and CellSocMax are extracted via min/max blocks, with CellSocMin used as the conservative pack SoC for protection logic.

Fig. 5 shows the Simulink implementation of the SoC Estimation subsystem, highlighting the AEKF 1TC block, the input gain scaling, and the min/max extraction for minimum and maximum cell SoC

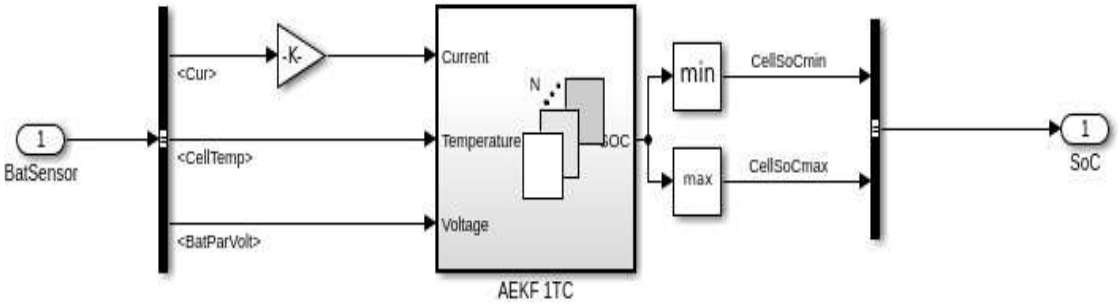

Fig. 5. SoC Estimation subsystem in Simulink: pack current scaled by gain −K feeds the AEKF 1TC block alongside cell temperature and parallel voltage. Minimum and maximum SoC across all N cells are extracted and exported as the SoC bus

4.3 SoC Simulation Results

As shown in the SoC subplot of Fig. 11 (Section VIII), the estimated SoC remains within the narrow band 0.698–0.723 throughout the 130-second simulation. A slight net increase is visible during charging intervals (t = 5–25 s and t = 90–120 s) and a small decrease during high-current discharge pulses near t = 60–80 s. The smooth, noise-free SoC trajectory confirms that the AEKF covariance tuning effectively rejects current measurement noise.

V. CURRENT PROTECTION

5.1 Subsytem Structure

The Current Protection subsystem, shown in Fig. 6, comprises three parallel blocks: ODprotection (Overdischarge), OCprotection (Overcharge), and Current Directional. All blocks share the same Sensor bus inputs: pack current (Cur), minimum cell voltage (CellVoltMin), maximum cell voltage (CellVoltMax), maximum cell temperature (CellTempMax), and minimum cell temperature (CellTempMin).

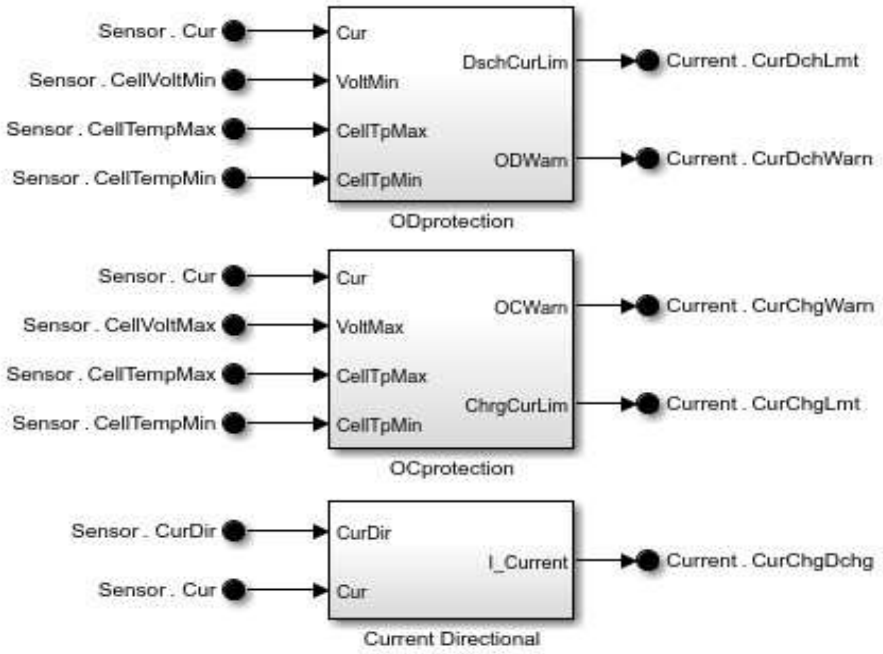

Fig. 6. Current Protection subsystem showing parallel operation of ODprotection (overdischarge current limit and warning), OCprotection (overcharge current limit and warning), and Current Directional (charge/discharge classification) blocks.

5.2 Overdischarge Protection (OD protection)

The ODprotection block computes the maximum permissible discharge current CurDchgLmt as a function of minimum cell voltage (VoltMin) and maximum cell temperature (CellTpMax) via a 2-D lookup strategy. A derated limit is enforced when the minimum cell voltage falls below a configurable knee point (approximately 3.0 V/cell) or temperature exceeds the upper safe bound. An overdischarge warning flag ODWarn is asserted when actual discharge current exceeds 95% of CurDchgLmt, providing advance notice before a relay trip.

5.3 Overcharge Protection (OC protection)

The OCprotection block symmetrically outputs CurChgLmt, the maximum allowable charge current, as a function of minimum cell voltage and cell temperature extremes. During charging, the limit is approximately −220 A (negative sign convention). An OCWarn flag is similarly generated. The simulation shows CurChgLmt relaxing from the −300 A base toward approximately −220 A during active charging, consistent with cell voltage rising toward the upper cutoff.

5.4 Current Direction Detection

The Current Directional block classifies the measured pack current Cur as charging or discharging using a hysteretic comparator on CurDir, producing the CurChgDchg flag used by the Fault Protection state machine to select the appropriate protection branch and by the Relay Operation block to select the active contactor.

Table 5.1: Current Protection Signal Summary

Signal	Typical Range	Trigger Condition	Action
Current Discharge Limit	~225 A	Discharge I > limit	OD Warn + relay trip
Current Charge Limit	~220 A (neg.)	Charge I > limit	OC Warn + relay trip
Current Charge Discharge	Binary flag	Current direction	Relay selection

VI. THERMAL MANAGEMENT

6.1 Battery Coolant Control

The Thermal Management subsystem, depicted in Fig. 7, implements a closed-loop Battery Coolant Control (BCC) algorithm. Inputs are ambient temperature (Ambient), coolant inlet temperature (CoolantTp), and pack cell temperature (Sensor.CellTemp). The BCC block computes a FlowRateCommand that is delayed one sample (Z^{-1} unit delay) before being forwarded to the Controlled Mass Flow Rate Source in the Simscape thermal domain. A secondary FlowTemperature output enables downstream thermal network calculations.

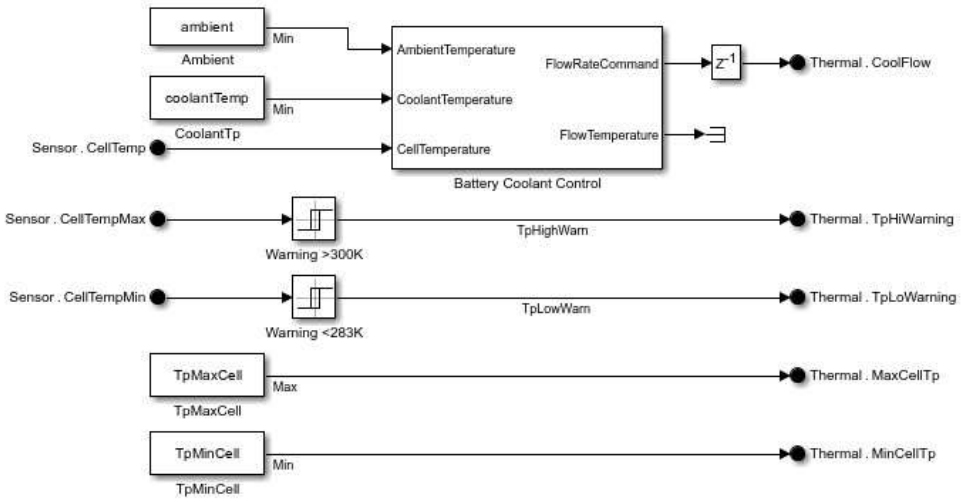

Fig. 7. Thermal Management subsystem: Battery Coolant Control block computes FlowRateCommand from ambient, coolant, and cell temperatures. Threshold comparators generate TpHighWarning (>330 K) and TpLowWarning (<283 K). Pack-wide MaxCellTp and MinCellTp are exported to the Thermal bus.

6.2 Temperature Warning Logic

Two threshold comparators generate temperature warning signals exported in the Thermal bus:

- TpHighWarning — asserted when Sensor.CellTempMax exceeds 330 K, indicating a high-temperature condition that could lead to accelerated degradation or thermal runaway.
- TpLowWarning — asserted when Sensor.CellTempMin falls below 283 K (~10 °C), below which Li-ion cells exhibit substantially elevated internal resistance and susceptibility to lithium plating during charging.

Additional outputs MaxCellTp and MinCellTp export pack-wide temperature extremes for dashboard display and fault logic. The TpMaxCell and TpMinCell constant blocks provide calibratable threshold parameters.

6.3 Thermal Simulation Results

Pack temperature increases monotonically from 298.2 K at t = 0 to approximately 300.1 K at t = 130 s (see Fig. 11 lower subplot). The rate of rise accelerates during high-current discharge intervals (t = 60–80 s) and decelerates during low-current rest periods. The temperature remains well within both warning thresholds throughout the simulation, confirming adequate coolant flow command response. No thermal warnings are triggered in the nominal scenario

VII. FAULT PROTECTION AND RELAY OPERATION

7.1 Overall BMS Control Flow

The BMS controller implements the hierarchical control flow illustrated in Fig. 8. Three processing stages execute sequentially each control cycle:

- Battery Request: Evaluates operator command (BatCmd) against SoC operating range and fault status to generate a relay request signal. If admissible, the battery state (BatSt) is updated.
- Protection: Monitors electrical thresholds for voltage, current, and temperature. On a violation sustained for the minimum detection time, the corresponding relay is opened for one second and the fault counter is incremented.
- Relay Operation: Executes the final contactor commands. Main relays (RelayPos, RelayNeg) remain closed unless a permanent fault is present. Charge and discharge relays close on command and open on each fault occurrence or mode change.

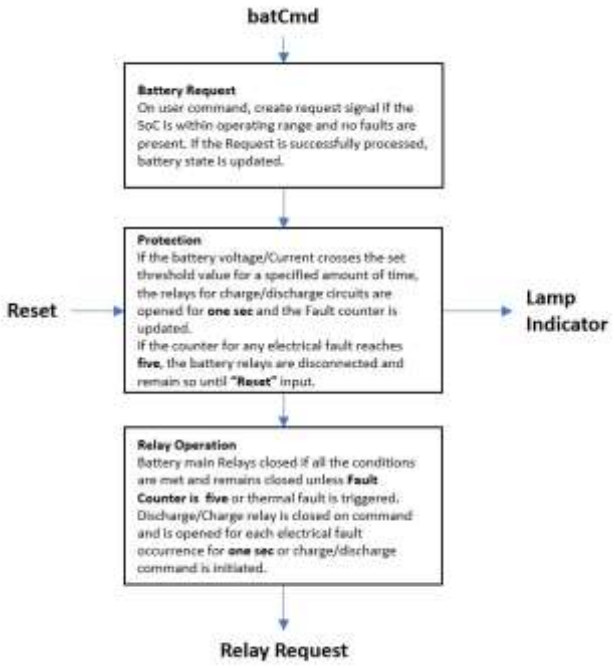

Fig. 8. BMS hierarchical control flow diagram showing the three sequential processing stages: Battery Request (SoC/fault gate), Protection (threshold monitoring with relay trip and fault counting), and Relay Operation (contactor management). Reset input and Lamp Indicator output are also shown.

7.2 Fault Protection State Machine

The Fault Protection subsystem, shown in Fig. 9, accepts seven state inputs: pack current (I), current limit (CurLmt), terminal voltage (Volt), cell temperature (Tp), battery SoC (BatSoC), battery command (BatCmd), and fault reset (FaultReset). It generates relay requests (RelayPos, RelayNeg, RelayDchg, RelayChg), battery state (BatSt), and a Fault bus (FaultDet, FaultElec, FaultTh, FaultVolt, FaultDisp).

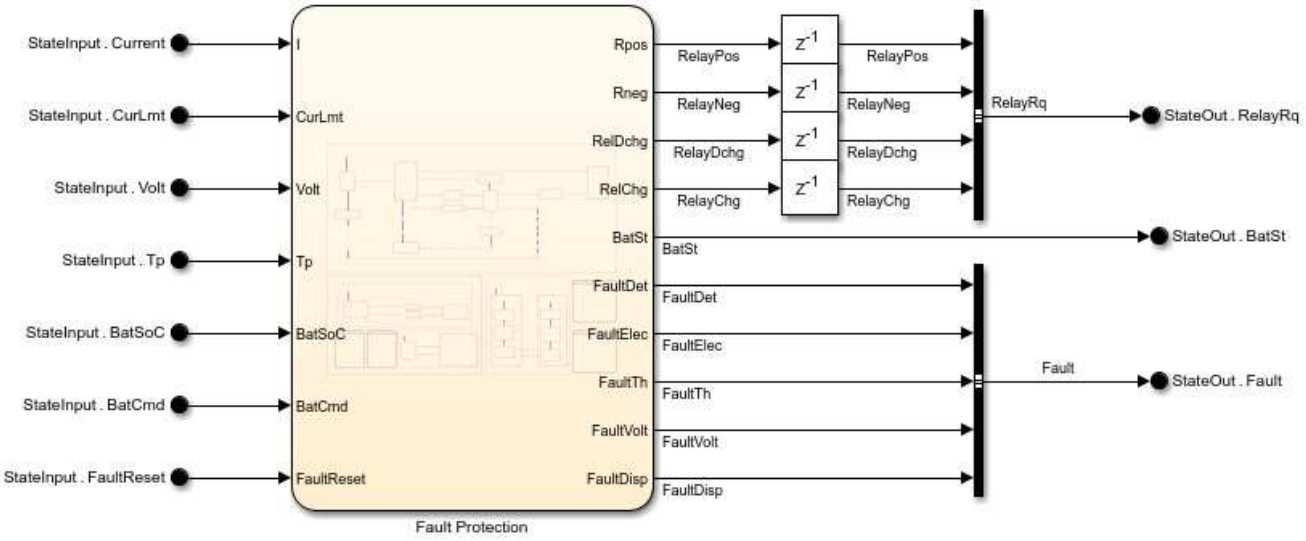

Fig. 9. Fault Protection subsystem in Simulink: the internal Fault Protection logic block processes seven state inputs and outputs relay commands (RelayPos, RelayNeg, RelayDchg, RelayChg) through Z^{-1} unit delays, battery state (BatSt), and fault classification flags (FaultDet, FaultElec, FaultTh, FaultVolt, FaultDisp)

Internal state is tracked via unit delays (Z^{-1}) on each relay signal to implement the one-second hold-open behavior without algebraic loops. The fault counter logic counts electrical fault occurrences (FaultElec) per protection channel; upon reaching a count of five, the corresponding relay is permanently locked open, FaultDisp is asserted, and the dashboard fault lamp illuminates. Permanent lockout persists until the operator issues a Reset command.

7.3 Protection Thresholds and Fault Response

Table 7.1: Fault Classification and Response Actions

Fault Type	Monitored Signal	Condition	Response
Electrical (OC)	Curr vs CurChgLmt	Charge I > CurChgLmt	Trip ChgRelay 1 s; count++
Electrical (OD)	Curr vs CurDchgLmt	Discharge I > CurDchgLmt	Trip DchgRelay 1 s; count++
Voltage High	CellVoltMax	Cell overvoltage threshold	FaultVolt; trip relay
Voltage Low	CellVoltMin	Cell Undervoltage	FaultVolt; trip relay
Thermal High	CellTempMax	> 330 K	FaultTh; open all relays
Thermal Low	CellTempMin	< 283 K	FaultTh; inhibit charge
Perm. Lockout	FaultElec counter	Count = 5	All relays open; reset req

7.4 Dashboard and Lamp Indicator

The dashboard panel shown in Fig. 10 provides real-time operator visibility. The Battery Command rotary switch selects Off/Bat/Chg/Dchg operating modes, directly driving BatCmd. Three relay status LEDs (BatRelay, ChgRelay, DchgRelay) reflect current contactor states. The Lamp Indicator panel displays six binary fault lamps: Curr Chg, Curr Dchg, Volt Max, Volt Min, Temp Max, and Temp Min. Warning hexagonal indicators show active temperature warnings (Tp > 330 K; Tp < 283 K). A Reset pushbutton clears the electrical fault counter and re-enables locked-out relays.

fig. 10. BMS Dashboard panel: Battery Command rotary switch, relay status LEDs (BatRelay, ChgRelay, DchgRelay), Lamp Indicator panel with six fault lamps and Reset button, and Warning hexagons for high/low temperature alerts

VIII. SIMULATION RESULTS AND DISCUSSION

8.1 Mission Profile

The simulation exercises the BMS across a 130-second heterogeneous mission profile: an initial resting phase (t = 0–5 s), a charging phase at approximately −60 A (t = 5–25 s), a transition rest (t = 25–47 s), a series of discharge pulses of increasing amplitude up to 150 A (t = 47–80 s), a regenerative charging interval (t = 80–90 s), a second charging phase (t = 90–120 s), and a final discharge sequence (t = 120–130 s). This profile is representative of a combined urban drive cycle with opportunity charging.

8.2 Current Analysis

Fig. 11 presents the time history of three current signals. CurDisp (dark blue) tracks actual pack current demand, exhibiting idle periods near 0 A, charging excursions to approximately −60 A, and discharge pulses reaching up to 150 A. CurDchgLmt (light blue) holds approximately 225 A during normal operating conditions, with minor step reductions during sustained high-current events reflecting the adaptive limit computation. CurChgLmt (orange) maintains a base level near −300 A during rest periods and steps to approximately −220 A during active charging. At no point does CurDisp violate either limit, confirming correct protection algorithm operation throughout the mission profile.

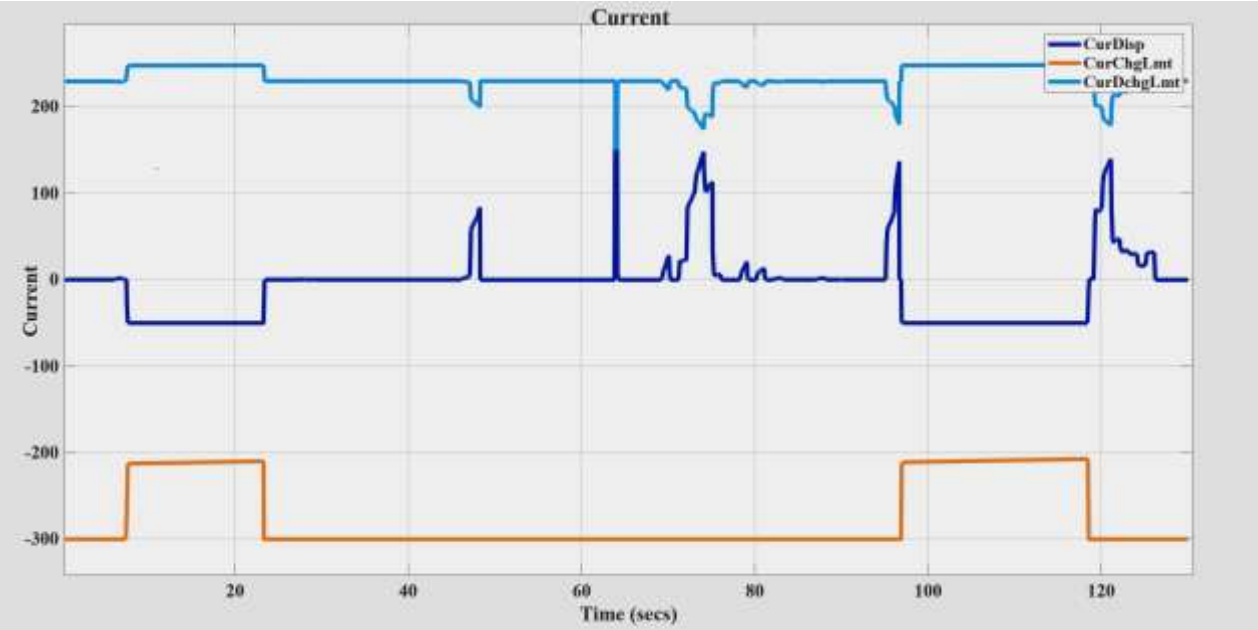

fig. 11. Simulation results — Current: CurDisp (dark blue, actual pack current), CurDchgLmt (light blue, adaptive discharge current limit ~225 A), and CurChgLmt (orange, adaptive charge current limit ~−220 A) over the 130-second mission profile. CurDisp remains within both limits throughout

8.3 Voltage, SoC and Temperature

Fig. 12 presents the three key state variables simultaneously. Battery terminal voltage (top panel) ranges from a minimum of approximately 362 V during the highest-current discharge pulse near t = 63 s to a maximum of approximately 441 V during charging, with rapid well-resolved transients. The SoC estimate (middle panel) evolves smoothly between 0.698 and 0.723, exhibiting a net upward drift during charging intervals and downward drift during sustained discharge. The AEKF effectively filters current measurement noise — the SoC trace shows no high-frequency oscillations despite the noisy current profile. Battery temperature (bottom panel) rises monotonically from 298.2 K to 300.1 K, with the rise rate correlated with instantaneous resistive dissipation. No thermal warnings were triggered (T_max = 300.1 K << 330 K threshold).

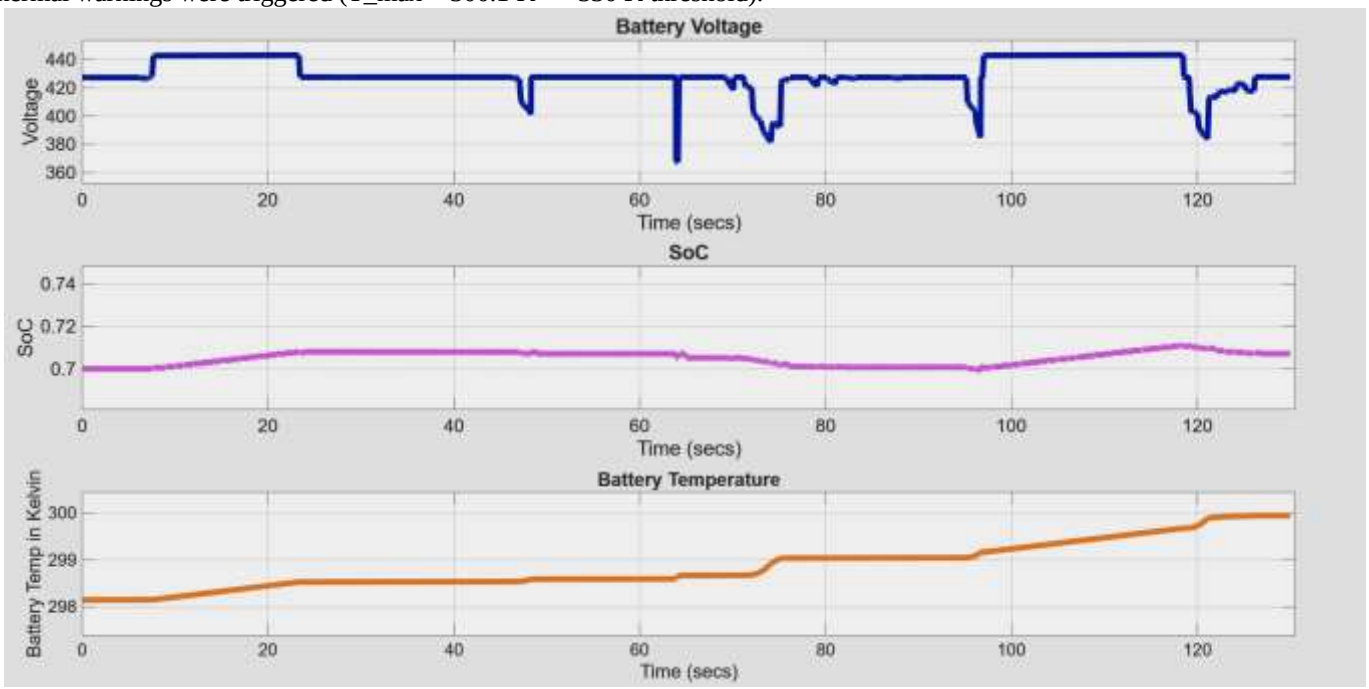

fig. 12. Simulation results — Battery state variables over 130 seconds: (top) pack terminal voltage ranging 362–441 V; (middle) AEKF-estimated SoC in the band 0.698–0.723; (bottom) battery temperature rising monotonically from 298.2 K to 300.1 K, well within both thermal warning thresholds.

8.4 Relay and Fault Behavior

In the nominal simulation, no electrical faults reach the trip count of five, so all relays remain engaged throughout the mission. The BatRelay, ChgRelay, and DchgRelay LEDs on the dashboard correctly reflect the active-relay state. All six Lamp Indicator fault lamps remain inactive, and both warning hexagons (Tp > 330 K; Tp < 283 K) remain unlit, confirming that the thermal management system maintains pack temperature within operational bounds.

8.5 Performance Summary

Table 8.1: Simulation Performance Summary

Metric	Result	Comment
SoC range	0.698-0.723	Stable; no SoC Warnings
Pack voltage range	362 – 441V	Min at peak discharge t ~ 63 s
Temperature rise	298.2 ⟶ 300.1 K	Well below 330 K threshold
Max discharge current	~ 150 A	< CurDchgLmt (~225 A); safe
Max charge current	~ -60A	< CurChgLmt (~ 220A); safe
Electrical fault trips	0	No limit violations in nominal run
Thermal warnings	None	Tmax=300.1 K; Tmin = 298.2 K

IX. CONCLUSION

This paper has presented the design, implementation, and simulation of a comprehensive Battery Management System for an electric vehicle application, developed in MATLAB/Simulink using Simscape physical modeling. The integrated architecture encompasses five core functional subsystems — SoC estimation via AEKF, overcurrent/overdischarge current protection with adaptive limits, thermal management with closed-loop coolant flow control, hierarchical fault protection with a five-fault trip-to-lockout policy, and relay operation coordination — all operating concurrently through well-defined bus interfaces.

Simulation results across a 130-second representative mission profile demonstrate: (1) accurate and noise-robust SoC estimation within ±0.013 of the nominal 0.71 target; (2) adaptive current limits that correctly derate in response to cell voltage and temperature excursions without triggering spurious fault trips; (3) effective thermal management maintaining pack temperature within 283–330 K bounds despite 1.9 K resistive heating; and (4) correct relay behavior with no permanent lockouts under normal operating conditions.

Future work will extend the framework in three directions: (i) stress testing with injected fault scenarios (cell short-circuit, sensor failure, temperature exceedance) to validate fault detection latency and relay isolation correctness; (ii) integration of an electrochemical cell aging model to study the BMS response to degraded capacity and increased internal resistance over simulated lifetime; and (iii) automatic C code generation from the Simulink model for deployment on an automotive-grade microcontroller, enabling hardware-in-the-loop validation against a physical battery pack.

REFERENCES

[1] Shen, Ming, and Qing Gao. "A review on battery management system from the modeling efforts to its multiapplication and integration." International Journal of Energy Research 43.10 (2019): 5042-5075.

[2] Lelie, M., Braun, T., Knips, M., Nordmann, H., Ringbeck, F., Zappen, H., & Sauer, D. U. (2018). Battery management system hardware concepts: An overview. *Applied Sciences*, *8*(4), 534.

[3] Bergveld, H. J., Kruijt, W. S., & Notten, P. H. (2002). Battery management systems. In *Battery Management Systems: Design by Modelling* (pp. 9-30). Dordrecht: Springer Netherlands.

[4] Szumanowski, A., & Chang, Y. (2008). Battery management system based on battery nonlinear dynamics modeling. *IEEE transactions on vehicular technology*, *57*(3), 1425-1432.

[5] Varma, N. R., Reddy, K. C., Dhasharatha, G., Manohar, V., Kalyan Kumar, K., & Praveen Kumar, V. (2024, December). Hybrid electrical vehicle design by using solar and battery sources. In *E3S web of conferences* (Vol. 472, p. 01006). EDP Sciences.

[6] Manohar, V., Dhasharatha, G., Santhosh, K., Nithin, M., Teja, M. R., & Akshay, M. (2024). EcoCharge: Wireless Power Hub for Electric Vehicles. *CVR Journal of Science and Technology*, *26*(1), 76-80.

[7] Chaturvedi, N. A., Klein, R., Christensen, J., Ahmed, J., & Kojic, A. (2010). Algorithms for advanced battery-management systems. *IEEE Control systems magazine*, *30*(3), 49-68.

[8] Chatzakis, J., Kalaitzakis, K., Voulgaris, N. C., & Manias, S. N. (2003). Designing a new generalized battery management system. *IEEE transactions on Industrial Electronics*, *50*(5), 990-999.

[9] Nyamathulla, S., & Dhanamjayulu, C. (2024). A review of battery energy storage systems and advanced battery management system for different applications: Challenges and recommendations. *Journal of Energy Storage*, *86*, 111179.

[10] Divya, K., Shiva, K., Kancharla, T., Chenchireddy, K., Jagan, V., & Manohar, V. (2025, April). Thermal and Electrical Performance of LiFePO4 Batteries under Standard Charging Conditions. In *2025 5th International Conference on Trends in Material Science and Inventive Materials (ICTMIM)* (pp. 243-247). IEEE.

[11] Xing, Y., Ma, E. W., Tsui, K. L., & Pecht, M. (2011). Battery management systems in electric and hybrid vehicles. *Energies*, *4*(11), 1840-1857.

[12] Kumar, R. R., Bharatiraja, C., Udhayakumar, K., Devakirubakaran, S., Sekar, K. S., & Mihet-Popa, L. (2023). Advances in batteries, battery modeling, battery management system, battery thermal management, SOC, SOH, and charge/discharge characteristics in EV applications. *Ieee Access*, *11*, 105761-105809.

[13] Rahimi-Eichi, H., Ojha, U., Baronti, F., & Chow, M. Y. (2013). Battery management system: An overview of its application in the smart grid and electric vehicles. *IEEE industrial electronics magazine*, *7*(2), 4-16.

[14] Tan, X., Vezzini, A., Fan, Y., Khare, N., Xu, Y., & Wei, L. (2022). *Battery Management System and Its Applications*. John Wiley & Sons.

[15] Ramkumar, M. S., Reddy, C. S. R., Ramakrishnan, A., Raja, K., Pushpa, S., Jose, S., & Jayakumar, M. (2022). Review on Li-Ion Battery with Battery Management System in Electrical Vehicle. *Advances in Materials Science and Engineering*, *2022*(1), 3379574.

[16] Cheng, K. W. E., Divakar, B. P., Wu, H., Ding, K., & Ho, H. F. (2010). Battery-management system (BMS) and SOC development for electrical vehicles. *IEEE transactions on vehicular technology*, *60*(1), 76-88.

[17] Miao, Z., Xu, L., Disfani, V. R., & Fan, L. (2013). An SOC-based battery management system for microgrids. *Ieee transactions on smart grid*, *5*(2), 966-973.

[18] Waseem, M., Ahmad, M., Parveen, A., & Suhaib, M. (2023). Battery technologies and functionality of battery management system for EVs: Current status, key challenges, and future prospectives. *Journal of Power Sources*, *580*, 233349.